CMA BLIND EQUALIZER FOR AERONAUTICAL TELEMETRY

Ding Xingwen   Zhai Wantao   Chang Hongyu   Chen Ming

Beijing Research Institute of Telemetry, China

ABSTRACT

In aeronautical telemetry, the multipath interference usually causes significant performance degradation. As the bit rate of telemetry systems increases, the impairments of multipath interference are more serious. The constant modulus algorithm (CMA) blind equalizer is effective to mitigate the impairments of multipath interference. The CMA adapts the equalizer coefficients to minimize the deviation of the signal envelope from a constant level. This paper presents the performances of the CMA blind equalizer applied for PCM-FM, PCM-BPSK, SOQPSK-TG and ARTM CPM in aeronautical telemetry.

KEY WORDS

Multipath Interference, Constant Modulus Algorithm, Blind Equalizer, PCM-FM, PCM-BPSK, SOQPSK-TG, ARTM CPM.

INTRODUCTION

It is widely recognized that the aeronautical telemetry channels are afflicted by multipath propagation effects [1][2]. Multipath generates inter-symbol and intra-symbol interference, which results in demodulation errors even at high Signal to Noise Ratio (SNR) and thus reduces the telemetry link availability. At low data rates, such as 100 kbps, the multipath interference appears as flat fading across the signal bandwidth. At high data rates, such as several Mbps, the signal bandwidth is much wider and the multipath interference is characterized by deep spectral nulls. So, as the bit rate of telemetry systems increases, the impairments of multipath interference are more serious.

The constant modulus algorithm (CMA) blind equalizer is effective to mitigate the impairments of multipath interference [3][4]. The CMA adapts the equalizer coefficients to minimize the deviation of the signal envelope from a constant level. The CMA blind equalizer has the advantage of being able to operate without a training sequence, even if the multipath interference is severe enough to close the eye pattern in the demodulator.

This paper presents the performances of the CMA blind equalizer applied for PCM-FM, PCM-BPSK, SOQPSK-TG and ARTM CPM in aeronautical telemetry.

CHANNEL MODELS FOR AERONAUTICAL TELEMETRY

As shown in Figure 1, practical telemetry situations have line-of-sight propagation with ample opportunity for specular reflections and diffuse scattering. Channel models are used to represent a mathematical description of these effects and to evaluate the performance of modulation, equalization and coding techniques on real channels. The channel impulse response is a function of the physical geometry involving the airborne transmitter, the receiver and the reflection points. Since this geometry varies during the telemetering mission, the channel impulse response is *time-variant*. It is assumed that over a short enough time interval, the channel does not change and is *time-invariant*. Thus, during a sufficiently short interval of time, the aeronautical telemetry channel can be modeled as a *linear*, *time-invariant* system with impulse response $h(t)$:

$$h(t) = \delta(t) + \sum_{k=1}^{L-1} \Gamma_k \exp(-j\omega_c \tau_k)\delta(t - \tau_k) \tag{1}$$

where Γ_k is the complex gain of the k-th propagation path relative to the line-of-sight signal, $0 \le |\Gamma_k| \le 1$, ω_c is the RF carrier frequency, τ_k is the delay of the k-th propagation path.

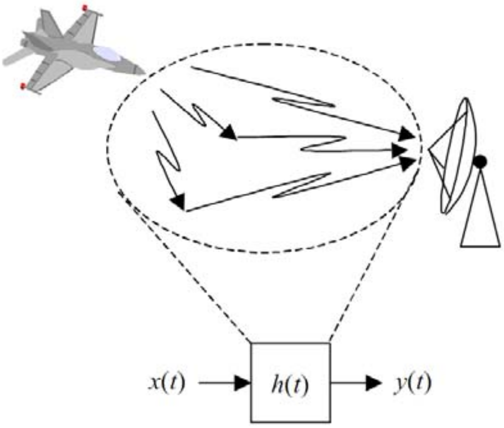

Figure 1. Channel models for aeronautical telemetry

The channel transfer function $H(\omega)$ is the Fourier transform of the channel impulse response $h(t)$. That is

$$H(\omega) = 1 + \sum_{k=1}^{L-1} \Gamma_k \exp(-j\omega_c \tau_k) \exp(-j\omega \tau_k) \qquad (2)$$

The channel transfer function $H(\omega)$ corresponding to the 2-ray channel model ($L = 2$) is illustrated in Figure 2(a). The transfer function is characterized by periodic nulls that occur every $1/\tau_1$ Hz. The depth of the null is determined by $|\Gamma_1|$. The frequency position of the null is determined by $\omega_c \tau_1 + \angle\Gamma_1$. Changes in $\angle\Gamma_1$ cause the frequency position of null to move, but not the periodic spacing. Changes in τ_1 will cause both the frequency position and the periodic spacing of the null to change. Note that when ω_c is large, even small changes in τ_1 can lead to huge changes in the frequency position of the null.

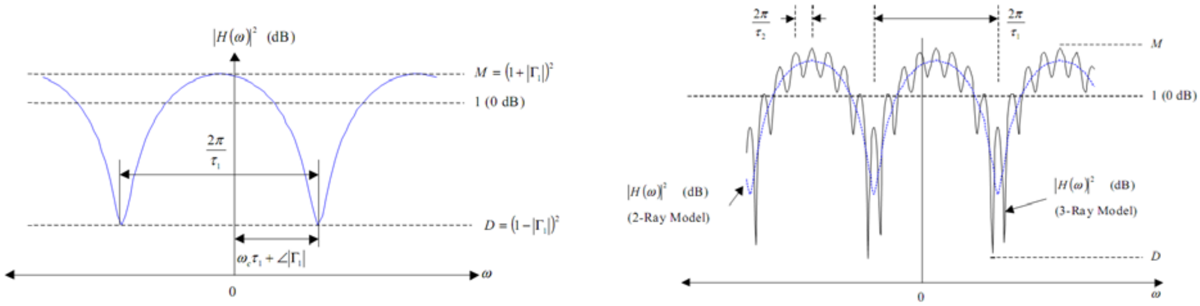

(a) The 2-ray channel model ($L = 2$) (b) The 3-ray channel model ($L = 3$)

Figure 2. Channel transfer function of channel model [5]

The channel transfer function corresponding to the 3-ray channel model ($L = 3$) is illustrated in Figure 2(b). In aeronautical telemetry, usually $|\Gamma_1| > |\Gamma_2|$ and $\tau_2 > \tau_1$. It means that the first propagation path is a strong short-delay reflection and the second propagation path is a weaker long-delay reflection. The effect of the additional second reflection in this case is to superimpose a “ripple” on the basic frequency response of the 2-ray model. The period of the “ripple” is determined by τ_2 and the amplitude of the “ripple” is determined by $|\Gamma_2|$. It has been shown that the 3-ray channel model ($L = 3$) can adequately capture all the essential features of the channel distortions caused by multipath propagation in aeronautical telemetry applications [2].

Channel models are usually categorized as either “narrowband” or “wideband” [6].

Narrowband channel models are appropriate when the signal bandwidth is much less than the coherence bandwidth of the multipath fading channel, so that the multipath fading process is frequency nonselective. For a narrowband signal, the multipath interference causes random fluctuations in the envelope of the received signal. M. Rice et al. [7] proposed a narrowband channel model for multipath fading in aeronautical telemetry applications. This narrowband channel model is composed of a line-of-sight signal, a specular reflection whose strength is 20% to 80% that of the line-of-sight signal, and a diffuse multipath component whose power is 10 to 20dB less than that of the line-of-sight signal. Thus the channel is close to AWGN (but not quite) with strong specular interference. Data collected from three test ranges is used to test the accuracy of this narrowband channel model.

Wideband channel models are used when the signal bandwidth is on the order of or larger than the coherence bandwidth of the multipath fading channel, so that the multipath fading process is frequency selective. M. Rice et al. [5][8] developed a wideband channel model for multipath fading in aeronautical telemetry applications. This wideband channel model is composed of three propagation paths: a line-of-sight path and two specular reflections. The first specular reflection is characterized by a relative amplitude of 70% to 96% of the line-of-sight amplitude and a delay of 10ns to 80 ns. The amplitude and delay of this path are defined completely by the flight path geometry. The second path is a much lower amplitude path with a longer delay. The gain of this path is well modeled as a zero-mean complex Gaussian random variable. The relative amplitude is approximately 2% to 8% of the line-of-sight amplitude. The mean excess delay is 155 ns with an RMS delay spread of 74 ns. Channel sounding data, collected at Edwards AFB, California at both L-Band and lower S-Band, were used to generate this wideband channel model.

This paper will concentrate on the wideband channel model for aeronautical telemetry. In the wideband channel model, the dominant feature of the multipath interference is the spectral null generated by the first multipath reflection. The time variations of this reflection depend on the flight path of the airborne transmitter and are slow enough to be tracked by an adaptive equalizer. The second multipath causes a small amplitude “ripple” in the channel transfer function that varies quickly with time. The changes in this “ripple” are probably too rapid to be tracked by an adaptive equalizer. Fortunately, the characteristic of the “ripple” is not the dominant multipath distortion on the aeronautical telemetry channels. So, we use the *2-ray wideband* channel model ($L = 2$) for the hardware experiments in this paper.

CMA BLIND EQUALIZER

Linear equalizers are attractive because they are mathematically tractable and may be implemented with low complexity. The CMA blind equalizer for aeronautical telemetry applications [9-12] is just a kind of linear adaptive equalizer. Because it is blind, it can operate without any knowledge of channel information, data symbols, phase synchronization or timing synchronization.

As shown in Figure 3, the CMA blind equalizer mitigates channel interference through application of a length-L FIR filter to the received signal before symbol detection,

$$y(n)=\sum_{l=0}^{L-1} w^{(n)}(l)r(n-l) \tag{3}$$

where $r(n)$ is the received signal, $y(n)$ is the output of the equalizer, $w^{(n)}(l)$ is the filter coefficients.

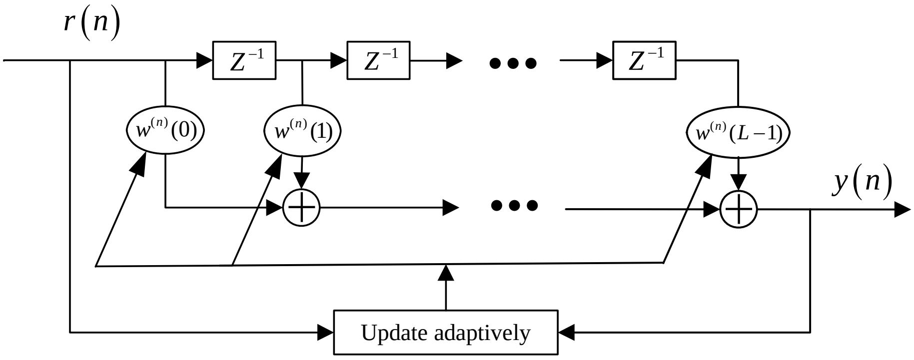

Figure 3. The structure of the CMA blind equalizer

Now we have implemented the CMA blind equalizer (with 24 taps) as an independent software module in the Field Programmable Gate Array (FPGA) device. The software module of the CMA blind equalizer can be used for all the common telemetry modulations with constant envelope, such as PCM-FM, PCM-BPSK, SOQPSK-TG and ARTM CPM. Since the CMA equalizer is “blind”, it can be “inserted” prior to the synchronization and the detector modules.

HARDWARE EXPERIMENTAL SCHEME

The traditional modulation methods for aeronautical telemetry are frequency modulation and phase modulation, such as PCM-FM and PCM-BPSK. When better bandwidth efficiency is required, the standard methods for digital signal transmission can be SOQPSK-TG and ARTM CPM [13]. Each of these methods offer constant envelope characteristics and are compatible with non-linear amplifiers with minimal spectral regrowth and minimal degradation of detection efficiency. So we choose PCM-FM, PCM-BPSK, SOQPSK-TG and ARTM CPM telemetry modulations for the hardware experiments of the CMA blind equalizer.

Since the dominant feature of the multipath interference is the spectral null generated by the first multipath reflection, we adopt the *2-ray wideband* channel model to simulate the multipath propagation, as illustrated in Figure 4. The modulation signal is transmitted into a demultiplexer to get two branches. One branch is modified on the power, phase and/or time delay, while the other branch is not changed. Then, the two branches are transmitted into a multiplexer to get a combined signal. It passes the Additive White Gaussian Noise (AWGN) channel to the receiver. In the receiver, the signal is first be handled by the CMA equalizer module (with 24 taps) before the demodulation. The demodulator of PCM-FM adopts the multi-symbol detection (MSD) [14]. The demodulator of PCM-BPSK adopts the conventional integrate and dump (I&D) detection. The demodulator of SOQPSK-TG adopts the pulse truncation (PT) detection ($L^{'}=1$) [15]. The demodulator of ARTM CPM adopts the pulse truncation (PT) detection ($L^{'}=2$) [16]. At last, we analyze the performances of the CMA equalizer by the bit error rate (BER) test.

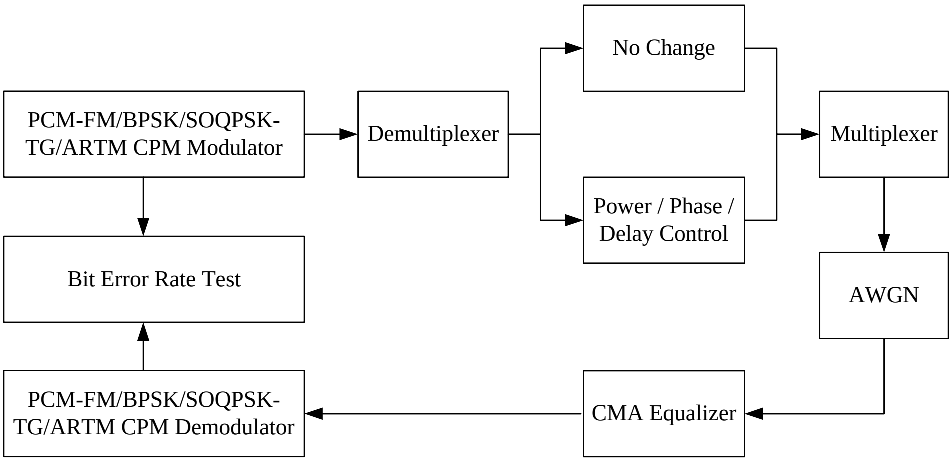

Figure 4. The hardware experimental scheme for the CMA blind equalizer

In the experiments, all the telemetry modulations are transmitted with the bit rate of 10Mbps and at the IF (intermediate frequency) of 70MHz. The parameters of the first multipath reflection are set as $\left|\Gamma_1\right| = 10\% \sim 90\%$, $\tau_1 = 100ns$. And $\angle\Gamma_1$ is changeable to ensure that the frequency position of null is at the middle of the frequency spectra of the signals, as shown in Figure 5 to Figure 8.

Figure 5 to Figure 8 respectively show the frequency spectra of 10 Mbps PCM-FM, PCM-BPSK, SOQPSK-TG and ARTM CPM signals at IF 70MHz, using the above hardware experimental scheme. All the left pictures are natural (without multipath), while all the right ones are fuzzy (due to the multipath interference).

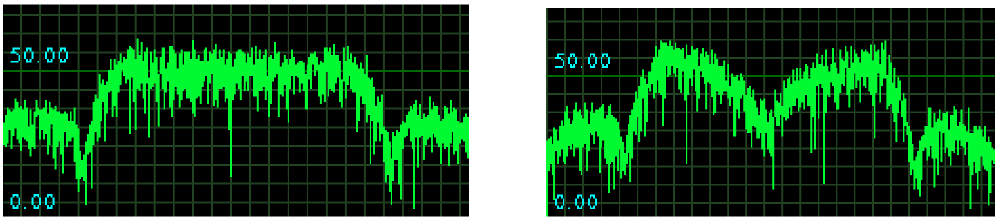

Figure 5. The frequency spectra of 10 Mbps PCM-FM
(Left : Without Multipath, Right : With Multipath)

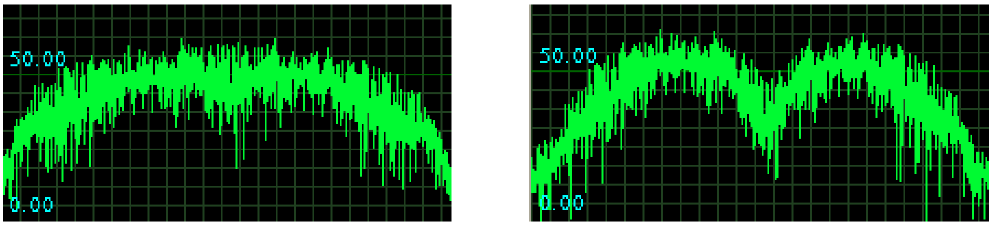

Figure 6. The frequency spectra of 10 Mbps PCM-BPSK
(Left : Without Multipath, Right : With Multipath)

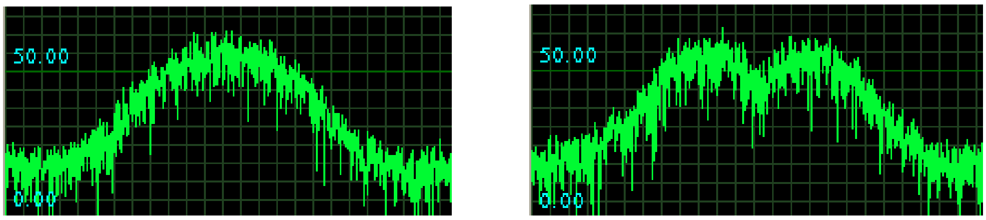

Figure 7. The frequency spectra of 10 Mbps SOQPSK-TG
(Left : Without Multipath, Right : With Multipath)

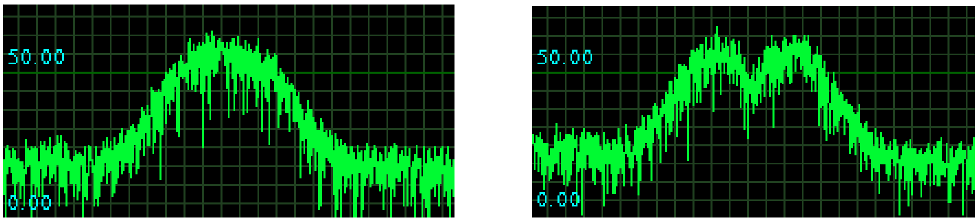

Figure 8. The frequency spectra of 10 Mbps ARTM CPM
(Left : Without Multipath, Right : With Multipath)

PERFORMANCE RESULTS AND ANALYSIS

Figure 9 to Figure 12 respectively show the BER experimental results of 10 Mbps PCM-FM, PCM-BPSK, SOQPSK-TG and ARTM CPM signals at IF 70MHz, using the above hardware experimental scheme. All the left pictures are the case of *Equalizer OFF* (with multipath), while all the right ones are the case of *Equalizer ON* (with *the same* multipath).

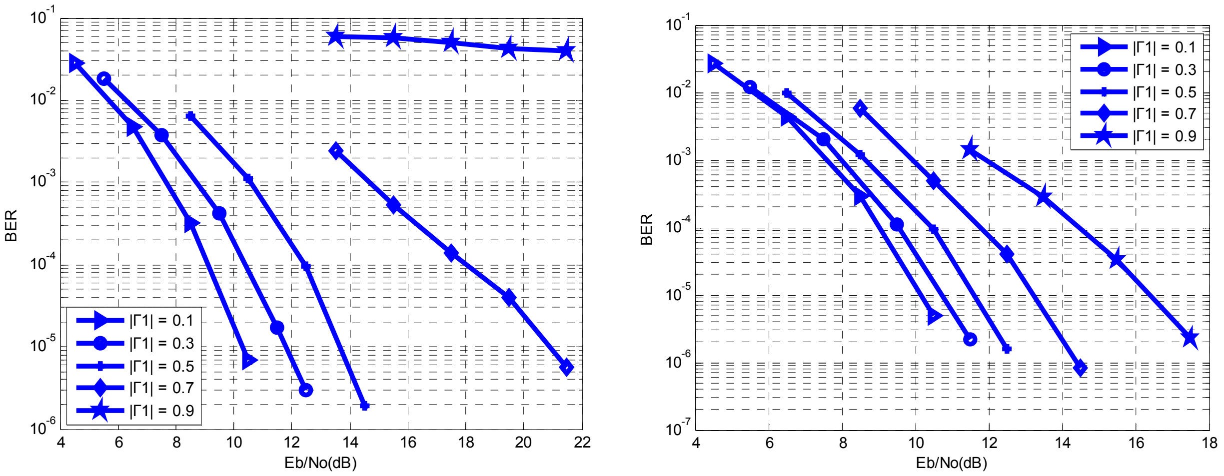

(a) Equalizer OFF (b) Equalizer ON

Figure 9. The performances of the CMA blind equalizer for 10 Mbps PCM-FM

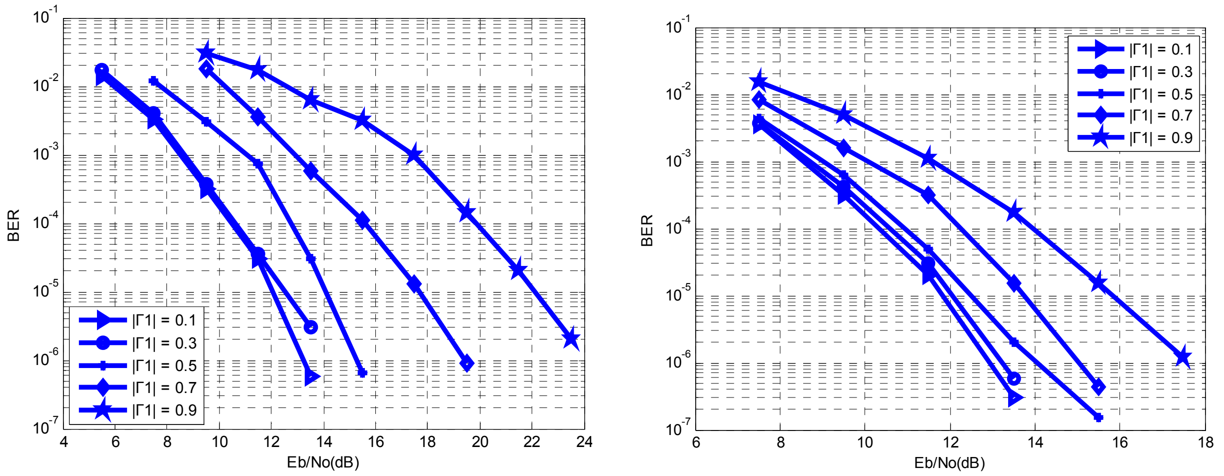

(a) Equalizer OFF (b) Equalizer ON

Figure 10. The performances of the CMA blind equalizer for 10 Mbps PCM-BPSK

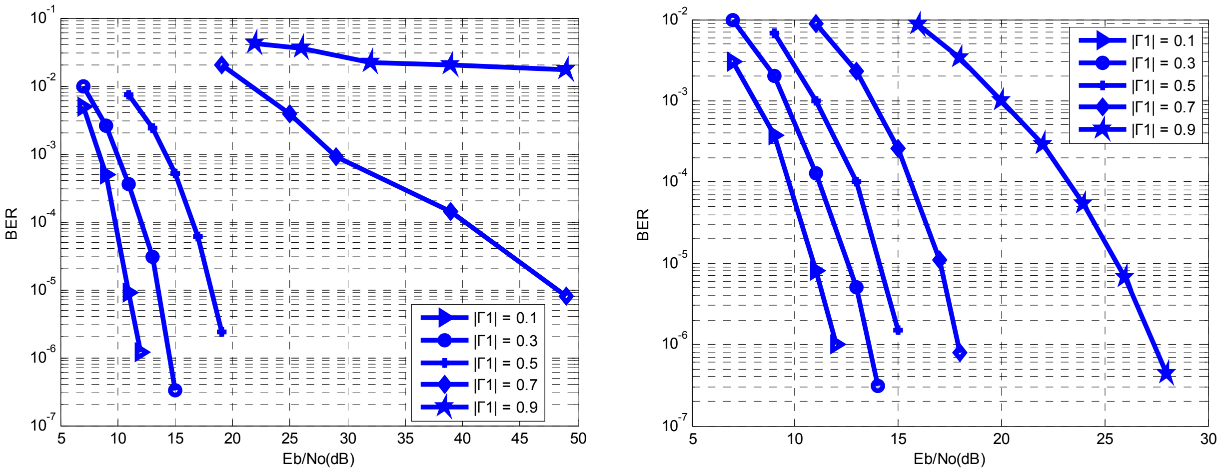

(a) Equalizer OFF (b) Equalizer ON

Figure 11. The performances of the CMA blind equalizer for 10 Mbps SOQPSK-TG

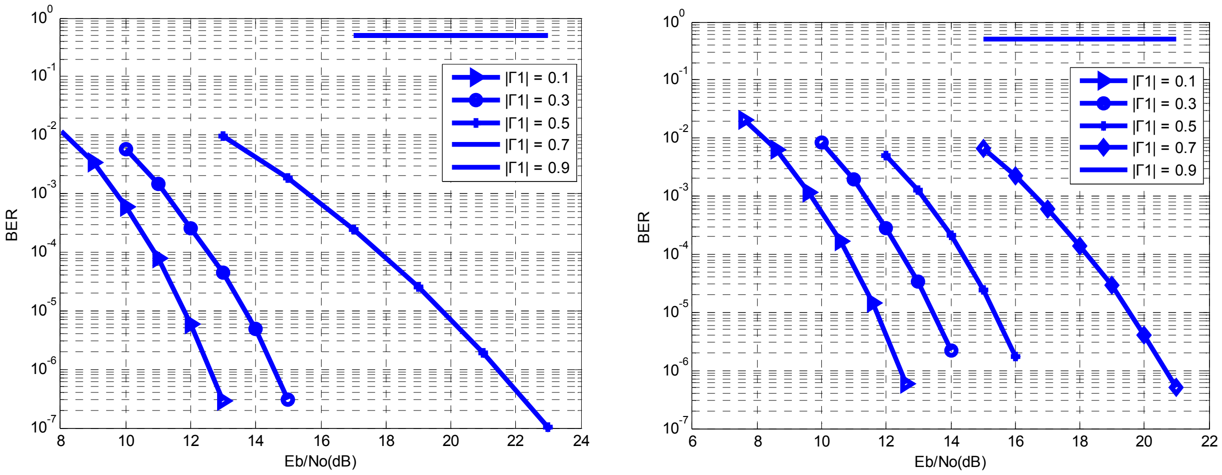

(a) Equalizer OFF (b) Equalizer ON

Figure 12. The performances of the CMA blind equalizer for 10 Mbps ARTM CPM

Table 1. The performance analysis of the CMA blind equalizer

Modulation type	The relative amplitude of the first specular reflection $\lvert\Gamma_1\rvert$	E_b/N_0(dB) required for BER = 10^{-5}		
		Equalizer OFF	Equalizer ON	Improved by the CMA blind equalizer
PCM-FM	0.1	10.2	10.1	0.1
	0.3	11.8	10.7	1.1
	0.5	13.6	11.6	2.0
	0.7	20.8	13.1	7.7
	0.9	----	16.3	>7.7
PCM-BPSK	0.1	12.0	11.8	0.2
	0.3	12.4	12.0	0.4
	0.5	14.1	12.5	1.6
	0.7	17.8	13.7	4.1
	0.9	22.1	15.8	6.3
SOQPSK-TG	0.1	10.9	10.8	0.1
	0.3	13.5	12.5	1.0
	0.5	18.1	14.1	4.0
	0.7	48.0	17.1	30.9
	0.9	----	25.5	>30.9
ARTM CPM	0.1	11.8	11.7	0.1
	0.3	13.6	13.4	0.2
	0.5	19.6	15.2	4.4
	0.7	----	19.5	>4.4
	0.9	----	----	----

Table 1 analyzes the performances of the CMA blind equalizer from the aspect of E_b/N_0(dB) required for BER = 10^{-5}, collecting data from Figure 9 to Figure 12. We can get the following conclusions:

- For all the telemetry modulations, the relative amplitude of the first specular reflection $\left|\Gamma_1\right|$ is greater, the BER is worse, whether *Equalizer OFF* or *Equalizer ON*.
- For all the telemetry modulations, the CMA blind equalizer is effective to mitigate the impairments of multipath interference. Generally, the relative amplitude of the first specular reflection $\left|\Gamma_1\right|$ is greater, the improved performance by the CMA blind equalizer is more obvious.
- The severe multipath interference may cause the phenomenon of the error floor. Fortunately, the CMA blind equalizer can solve the error floor effectively, as shown in Figure 9 (in the case of $\left|\Gamma_1\right| = 0.9$), Figure 11 (in the case of $\left|\Gamma_1\right| = 0.9$) and Figure 12 (in the case of $\left|\Gamma_1\right| = 0.7$). But, if the multipath interference is severe awfully, the CMA blind equalizer may be noneffective for certain modulation, as shown in Figure 12 (in the case of $\left|\Gamma_1\right| = 0.9$).
- Among the four types of telemetry modulations, ARTM CPM is the most sensitive to the severe multipath interference ($\left|\Gamma_1\right| > 0.7$).

CONCLUSIONS

In aeronautical telemetry, the multipath interference usually causes significant performance degradation. The channel models for aeronautical telemetry with multipath interference are introduced. Then, we emphatically present the performances of the CMA blind equalizer applied for PCM-FM, PCM-BPSK, SOQPSK-TG and ARTM CPM telemetry signals. The hardware experimental results prove that the CMA blind equalizer is effective to mitigate the impairments of multipath interference for aeronautical telemetry.

REFERENCES

[1] M. Rice and E. Law, “Aeronautical Telemetry Fading Sources at Test Ranges,” Proceedings of the International Telemetering Conference, Las Vegas, NV, October 1997.

[2] M. Rice, D. de Gaston, A. Davis, G. German and C. Bettwieser, “ARTM channel sounding results — An investigation of frequency selective fading on aeronautical telemetry channels,” Proceedings of the International Telemetering Conference, Las Vegas, NV, October 1999.

[3] J. Treichler and B. Agee, “A new approach to multipath correction of constant modulus signals,” IEEE Transactions on Acoustics, Speech, and Signal Processing, Vol. 31, No. 2, April 1983, 459-472.

[4] J. Treichler and M. Larimore, “New processing techniques based on the constant modulus adaptive algorithm,” IEEE Transactions on Acoustics, Speech, and Signal Processing, Vol. 33, No. 2, April 1985, 420–431.

[5] M. Rice, A. Davis and C. Bettwieser, “A Wideband Channel Model for Aeronautical Telemetry - Part 1: Geometric Considerations and Experimental Configuration,” Proceedings of the International Telemetering Conference, San Diego, CA, October 2002.

[6] John G. Proakis and Masoud Salehi, Digital Communications, fifth edition, McGraw-Hill, New York, 2008.

[7] M. Rice, R. Dye and K. Welling, “Narrowband channel model for aeronautical telemetry,” IEEE Transactions on Aerospace and Electronic Systems, Vol. 36, No. 4, October 2000, 1090-1098.

[8] M. Rice, A. Davis and C. Bettwieser, “A Wideband Channel Model for Aeronautical Telemetry - Part 2: Modeling Results,” Proceedings of the International Telemetering Conference, San Diego, CA, October 2002.

[9] Zhong Ye, E. H. Satorius, T. C. Jedrey and K. Temple, “Enhancement of Advanced Range Telemetry (ARTM) Channels via Blind Equalization,” Proceedings of the International Telemetering Conference, Las Vegas, NV, October 2001.

[10] T. Hill and M. Geoghegan, “A comparison of adaptively equalized PCM/FM, SOQPSK, and Multi-h CPM in a multipath environment,” Proceedings of the International Telemetering Conference, San Diego, CA, October 2002.

[11] M. Geoghegan, “Experimental Results for PCM/FM, Tier I SOQPSK, and Tier II Multi-h CPM with CMA Equalization,” Proceedings of the International Telemetering Conference, Las Vegas, NV, October 2003.

[12] M. Rice and E. Satorius, “A Comparison of MMSE and CMA Equalization Techniques for ARTM Tier-I Waveforms,” Proceedings of the International Telemetering Conference, San Diego, CA, October 2004.

[13] Telemetry Group, Telemetry Standards, IRIG Standard 106-15 (Part 1), Range Commanders Council, US Army White Sands Missile Range, New Mexico, July 2015. Available: http://jcs.mil/RCC/manuals/106-15.

[14] M. Geoghegan, “Improving the Detection Efficiency of Conventional PCM/FM Telemetry by using a Multi-Symbol Demodulator,” Proceedings of the International Telemetering Conference, San Diego, CA, October 2000.

[15] Ding Xingwen, Zhai Wantao, Song Jianyong and Chen Ming, “A Comparison of Coherent Detectors for SOQPSK-TG,” Proceedings of the International Telemetering Conference, Las Vegas, NV, October 2015.

[16] E. Perrins and M. Rice, “Reduced Complexity Detectors for Multi-h CPM in Aeronautical Telemetry,” IEEE Transactions on Aerospace and Electronic Systems, Vol. 43, No. 1, January 2007, 286-300.